Available online at www.sciencedirect.com
SCIENCE DIRECT®
International Journal of Engineering Science 42 (2004) 571–590
International Journal of Engineering Science
www.elsevier.com/locate/ijengsci

Biomagnetic channel flow in spatially varying magnetic field

V.C. Loukopoulos [a], E.E. Tzirtzilakis [b,*]

[a] Department of Physics, University of Partas, 26500 Patras, Greece
[b] Division of Applied Analysis, Department of Mathematics, University of Partas, 26500 Patras, Greece

Received 24 March 2003; received in revised form 2 June 2003; accepted 30 July 2003

Abstract

In this work the fundamental problem of the biomagnetic fluid flow in a channel under the influence of an applied magnetic field is studied. It is assumed that the magnetization M of the fluid is varying linearly with temperature T and magnetic field intensity H. For the numerical solution of the problem, which is described by a coupled and non-linear system of PDEs, with their appropriate boundary conditions, the stream function–vorticity formulation is adopted. The solution of the problem is obtained developing an efficient numerical technique based on finite differences. This technique assures that in the algebraic system arising after discretization, the matrix of the unknowns is diagonally dominant. Results concerning the velocity and temperature field, skin friction and rate of heat transfer indicate that the presence of magnetic field appreciable influence the flow field. A vortex is arising near the lower plate below of which the magnetic source is placed. The temperature, as well as the skin friction and the rate of heat transfer are increasing in the same area.

Keywords: Blood; Biofluid; Magnetic field; Fluid mechanics; BFD; Non-conducting

1. Introduction

Biomagnetic fluid dynamics (BFD) is a relatively new area in fluid mechanics investigating the fluid dynamics of biological fluids in the presence of magnetic field. The applications in bioengineering and medicine seem to be numerous and the research work is rapidly growing [1–7].

Mathematical models have been developed in order to examine the flow of a biomagnetic fluid under the action of an applied magnetic field. The implementation of these models is based on the

* Corresponding author. Tel./fax: +30-2610997396.
E-mail address: stratis@math.upatras.gr (E.E. Tzirtzilakis).

0020-7225/$ - see front matter
doi:10.1016/j.ijengsci.2003.07.007

modified Stokes principles and on the assumption that besides the three thermodynamic variables P, ρ and T the biomagnetic fluid behavior is also a function of magnetization M [8,9]. Magnetization is the measure of how much the magnetic field is affecting the magnetic fluid and generally is a function of the magnetic field intensity H and the temperature T.

Unlike magnetohydrodynamics (MHD), which deals with conducting fluids, the mathematical model of BFD ignores the effect of polarization and magnetization and the induced current is negligibly small. Thus in BFD, unlike MHD, Lorentz force is much smaller in comparison to the magnetization force. According to the above mentioned mathematical model biofluids are considered poor conductors and the flow is affected only by the magnetization of the fluid in the magnetic field.

The derived governing equations for incompressible fluid flow are similar to those derived for ferrohydrodynamics (FHD) [10–16].

The most characteristic biomagnetic fluid is the blood, which can be considered as a magnetic fluid because the red blood cells contain the hemoglobin molecule, a form of iron oxides, which is present at a uniquely high concentration in the mature red blood cells. It is found that the erythrocytes orient with their disk plane parallel to the magnetic field [17–20] and also that the blood possesses the property of diamagnetic material when oxygenated and paramagnetic when deoxygenated [21].

So, blood possesses the property of a magnetic material, and under some circumstances, can be considered as diamagnetic or paramagnetic fluid [8].

In the present study a simplification of this mathematical model of BFD is used to obtain numerical solution of the differential equations describing the fluid flow (blood) in a rectangular channel under the action of a magnetic field.

It is assumed that the flow is two-dimensional, laminar, incompressible, and the magnetization is described by a linear equation involving the magnetic intensity H and temperature T. The two impermeable plates of the channel are kept at different constant temperature and as far as concerns the magnetic field it is assumed equilibrium flow. The Biofluid considered is blood and as a simplification Newtonian behavior is assumed.

In order to proceed to the numerical solution the stream function–vorticity formulation is adopted and the solution of the problem is obtained numerically developing an efficient numerical technique using finite differences. This technique assures that in the algebraic system arising after discretization, the matrix of the unknowns is diagonally dominant.

The results concerning the velocity and temperature field, skin friction and rate of heat transfer presented, showed that the flow is appreciably influenced by the magnetic field. A vortex is arising and the temperature is increasing near the area where the source is located. These results indicate that application of a magnetic field, in the flow of a biomagnetic fluid, could be useful for medical and engineering applications.

2. Mathematical formulation

The viscous, steady, two-dimensional, incompressible, laminar biomagnetic fluid (blood) flow is considered taking place between two parallel flat plates (channel). The length of the plates is $\bar{L}$ and the distance between them is $\bar{h}$, such that $\bar{L}/\bar{h} = 10$. The flow at the entrance is assumed to be fully

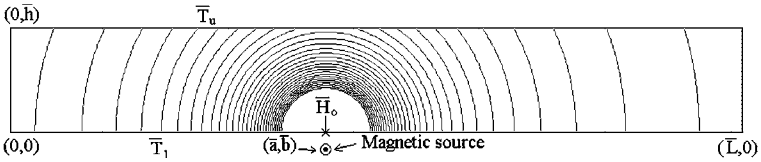

Fig. 1. Flow domain and contours of the magnetic field strength H.

developed and the upper plate is kept at constant temperature $\overline{T}_{\mathrm{u}}$, while the lower at $\overline{T}_{\mathrm{l}}$, such that $\overline{T}_{\mathrm{l}} < \overline{T}_{\mathrm{u}}$. The origin of the Cartesian coordinate system is located at the leading edge of the lower plate and the flow is subjected to a magnetic source, which is placed very close to the lower plate and below it (see Fig. 1).

Blood is considered as electrically non-conducting biomagnetic fluid [4,8,9] and Newtonian behavior is assumed as in [22,23]. The rotational forces acting on the erythrocytes when entering the magnetic field are discarded (equilibrium flow).

The governing equations of the fluid flow, under the action of the applied magnetic field, are similar to those derived in FHD [4,8,9,13,15]. Hence at the channel flow the dimensional velocity components of $\vec{q} = (\bar{u}, \bar{v})$ the pressure $\bar{p}$ and the temperature $\overline{T}$ are governed by the mass conservation, the fluid momentum equations at the $\bar{x}, \bar{y}$ directions, and the energy equation, which are given respectively by

$$\frac{\partial \bar{u}}{\partial \bar{x}} + \frac{\partial \bar{v}}{\partial \bar{y}} = 0, \tag{1}$$

$$\bar{\rho}\left(\bar{u}\frac{\partial \bar{u}}{\partial \bar{x}} + \bar{v}\frac{\partial \bar{u}}{\partial \bar{y}}\right) = -\frac{\partial \bar{p}}{\partial \bar{x}} + \bar{\mu}_0 \overline{M}\frac{\partial \overline{H}}{\partial \bar{x}} + \bar{\mu}\left(\frac{\partial^2 \bar{u}}{\partial \bar{x}^2} + \frac{\partial^2 \bar{u}}{\partial \bar{y}^2}\right), \tag{2}$$

$$\bar{\rho}\left(\bar{u}\frac{\partial \bar{v}}{\partial \bar{x}} + \bar{v}\frac{\partial \bar{v}}{\partial \bar{y}}\right) = -\frac{\partial \bar{p}}{\partial \bar{y}} + \bar{\mu}_0 \overline{M}\frac{\partial \overline{H}}{\partial \bar{y}} + \bar{\mu}\left(\frac{\partial^2 \bar{v}}{\partial \bar{x}^2} + \frac{\partial^2 \bar{v}}{\partial \bar{y}^2}\right), \tag{3}$$

$$\begin{aligned}&\bar{\rho}\bar{c}_p\left(\bar{u}\frac{\partial \overline{T}}{\partial \bar{x}} + \bar{v}\frac{\partial \overline{T}}{\partial \bar{y}}\right) + \bar{\mu}_0 \overline{T}\frac{\partial \overline{M}}{\partial \overline{T}}\left(\bar{u}\frac{\partial \overline{H}}{\partial \bar{x}} + \bar{v}\frac{\partial \overline{H}}{\partial \bar{y}}\right)\\ &\quad = \bar{k}\left(\frac{\partial^2 \overline{T}}{\partial \bar{x}^2} + \frac{\partial^2 \overline{T}}{\partial \bar{y}^2}\right) + \bar{\mu}\left[2\left(\frac{\partial \bar{u}}{\partial \bar{x}}\right)^2 + 2\left(\frac{\partial \bar{v}}{\partial \bar{y}}\right)^2 + \left(\frac{\partial \bar{v}}{\partial \bar{x}} + \frac{\partial \bar{u}}{\partial \bar{y}}\right)^2\right].\end{aligned} \tag{4}$$

The boundary conditions of the problem are

$$\left.\begin{array}{lll}\text{Inflow} & (\bar{x} = 0, 0 \leqslant \bar{y} \leqslant \bar{h}): & \bar{u} = \bar{u}(\bar{y}),\ \bar{v} = 0,\ \overline{T} = \overline{T}(\bar{y}),\\ \text{Outflow} & (\bar{x} = \bar{L}, 0 \leqslant \bar{y} \leqslant \bar{h}): & \partial(\bar{R})/\partial \bar{x} = 0,\\ \text{Upper plate} & (\bar{y} = \bar{h}, 0 \leqslant \bar{x} \leqslant \bar{L}): & \bar{u} = 0,\ \bar{v} = 0,\ \overline{T} = \overline{T}_{\mathrm{u}},\\ \text{Lower plate} & (\bar{y} = 0, 0 \leqslant \bar{x} \leqslant \bar{L}): & \bar{u} = 0,\ \bar{v} = 0,\ \overline{T} = \overline{T}_{\mathrm{l}}.\end{array}\right\} \tag{5}$$

In the above equations $\bar{u}(\bar{y})$ is a parabolic velocity profile corresponding to fully developed flow, $\overline{T}(\bar{y})$ is a linear profile, $\bar{R}$ stands for $\overline{T}$, $\bar{u}$ or $\bar{v}$, $\bar{\rho}$ is the biomagnetic fluid density, $\bar{\mu}$ is the dynamic viscosity, $\bar{\mu}_0$ is the magnetic permeability of vacuum, $\bar{c}_p$ the specific heat at constant pressure, $\bar{k}$ the thermal conductivity, $\overline{T}$ the temperature and the bar above the quantities denotes that they are dimensional.

The terms $\bar{\mu}_0\overline{M}\,\partial\overline{H}/\partial\bar{x}$ and $\bar{\mu}_0\overline{M}\,\partial\overline{H}/\partial\bar{y}$ in (2) and (3), respectively, represent the components of the magnetic force, per unit volume, and depend on the existence of the magnetic gradient.

The term $\bar{\mu}_0\overline{T}\frac{\partial\overline{M}}{\partial\overline{T}}\left(\bar{u}\frac{\partial\overline{H}}{\partial\bar{x}}+\bar{v}\frac{\partial\overline{H}}{\partial\bar{y}}\right)$ of Eq. (4) represents the thermal power per unit volume due to the magnetocaloric effect.

According to FHD the magnetization $\overline{M}$, under the equilibrium assumption, is generally a function of the magnetic field strength $\overline{H}$, temperature $\overline{T}$ and fluid density $\bar{\rho}$ [13,15]. In the present formulation, as well as in that of BFD, the blood is actually considered as electrically non-conducting magnetic fluid. Thus, for the variation of magnetization $\overline{M}$, with the magnetic field intensity $\overline{H}$ and temperature $\overline{T}$, the following relation, derived experimentally for a magnetic fluid [24], is considered.

$$\overline{M}=\overline{KH}(\overline{T}_{\mathrm{c}}-\overline{T}),\tag{6}$$

where $\overline{K}$ is a constant and $\overline{T}_{\mathrm{c}}$ is the Curie temperature [24].

For the expression of the magnetic field strength it can be considered that the magnetic source represents a magnetic wire placed vertically to the $\bar{x}$–$\bar{y}$ plane at the point $(\bar{a},\bar{b})$. The magnetic field intensity $\overline{H}(\bar{x},\bar{y})$ of such magnetic wire is given by the expression [15]

$$\overline{H}(\bar{x},\bar{y})=\frac{\bar{\gamma}}{2\pi}\frac{1}{(\bar{x}-\bar{a})^2+(\bar{y}-\bar{b})^2},\tag{7}$$

where $\bar{\gamma}$ is the magnetic field strength at the source (of the wire) and $(\bar{a},\bar{b})$ is the position where the source is located. The contours of the magnetic field strength are shown in Fig. 1.

3. Transformation of equations

In order to proceed to the numerical solution of the system (1)–(4) with boundary conditions (5) and the assumptions (6) and (7), the following non-dimensional variables are introduced

$$x=\frac{\bar{x}}{\bar{h}},\quad y=\frac{\bar{y}}{\bar{h}},\quad u=\frac{\bar{u}}{\bar{u}_r},\quad v=\frac{\bar{v}}{\bar{u}_r},\tag{8}$$

$$p=\frac{\bar{p}}{\rho\bar{u}_r^2},\quad H=\frac{\overline{H}}{\overline{H}_r},\quad T=\frac{\overline{T}_{\mathrm{u}}-\overline{T}}{\overline{T}_{\mathrm{u}}-\overline{T}_1},\tag{9}$$

where, $\bar{u}_r$ is the maximum velocity at the entrance and $\overline{H}_r$ is the magnetic field strength at the point $(a,b)=(2.5,0)$, whereas the source is placed at the point $(a,b)=(2.5,-0.05)$. The contours of the dimensionless magnetic field strength H are shown in Fig. 1.

In order to eliminate the pressure and reduce the number of equations of the system (1)–(4) the stream function–vorticity formulation is adopted, by introducing the dimensionless vorticity function $J = J(x, y)$ and the dimensionless stream function $\Psi = \Psi(x, y)$ defined by the expressions

$$J(x,y) = \frac{\partial v}{\partial x} - \frac{\partial u}{\partial y}, \tag{10}$$

$$u = \frac{\partial \Psi}{\partial y}, \quad v = -\frac{\partial \Psi}{\partial x}. \tag{11}$$

Thus, Eq. (1) is automatically satisfied and Eqs. (2)–(4) produce, by eliminating the pressure p from the first two and substituting (11) in (4) and (10), the following system of equations

$$\nabla^2 \Psi = -J, \tag{12}$$

$$\nabla^2 J = Re\left\{\frac{\partial J}{\partial x}\frac{\partial \Psi}{\partial y} - \frac{\partial J}{\partial y}\frac{\partial \Psi}{\partial x}\right\} + Mn\,Re\,H\left\{\frac{\partial H}{\partial x}\frac{\partial T}{\partial y} - \frac{\partial H}{\partial y}\frac{\partial T}{\partial x}\right\}, \tag{13}$$

$$\begin{aligned}\nabla^2 T = {} & Pr\,Re\left\{\frac{\partial T}{\partial x}\frac{\partial \Psi}{\partial y} - \frac{\partial T}{\partial y}\frac{\partial \Psi}{\partial x}\right\} + Mn\,Pr\,Re\,Ec\,H(\varepsilon - T)\left\{\frac{\partial H}{\partial x}\frac{\partial T}{\partial y} - \frac{\partial H}{\partial y}\frac{\partial T}{\partial x}\right\} \\ & + Pr\,Ec\left\{\left(\frac{\partial^2 \Psi}{\partial y^2} - \frac{\partial^2 \Psi}{\partial x^2}\right)^2 + 4\left(\frac{\partial^2 \Psi}{\partial x \partial y}\right)^2\right\},\end{aligned} \tag{14}$$

where ∇^2 is the two-dimensional Laplacian operator ($\nabla^2 = \vec{\nabla} \cdot \vec{\nabla} = (\partial^2/\partial x^2 + \partial^2/\partial y^2)$).

The non-dimensional parameters entering now into the problem under consideration are

$$Re = \frac{\bar{h}\bar{\rho}\bar{u}_r}{\bar{\mu}} \text{ (Reynolds number)}, \quad Mn = \frac{\bar{\mu}_0 \overline{H}_r^2 \overline{K}(\overline{T}_{\mathrm{u}} - \overline{T}_1)}{\bar{\rho}\bar{u}_r^2} \text{ (Magnetic number)},$$

$$\varepsilon = \frac{\overline{T}_{\mathrm{u}}}{\overline{T}_{\mathrm{u}} - \overline{T}_1} \text{ (Temperature number)}, \quad Pr = \frac{\bar{c}_p \bar{\mu}}{\bar{k}} \text{ (Prandtl number)},$$

$$Ec = \frac{\bar{u}_r^2}{\bar{c}_p(\overline{T}_{\mathrm{u}} - \overline{T}_1)} \text{ (Eckert number)}.$$

The new parameter entering into the problems of BFD is the magnetic number Mn defined above and expresses the ratio of magnetic to the inertia forces.

It is worth mentioning here that when the magnetic number $Mn = 0$ the problem is a common hydrodynamic flow in a channel with heat transfer. Also, for a specific Reynolds number ($\bar{u}_r = \text{const.}$) increasing Mn is equivalent either increasing the magnetic field strength $\overline{H}_r$ at the point $(2.5, 0)$, or the temperature difference between the two plates.

3.1. Boundary conditions

The system of equations (12)–(14) is of elliptic type and boundary conditions, for the unknown functions Ψ, J and T, are required. The boundary for the problem under consideration is the one shown in Fig. 1, e.g. the rectangular OABC with O$(0,0)$, A$(\bar{L},0)$, B$(\bar{L},\bar{h})$ and C$(0,\bar{h})$. After the introduction of the non-dimensional coordinates these coordinates are transformed to $(0,0)$, $(10,0)$, $(10,1)$ and $(0,1)$, respectively.

All unknown quantities at the exit of the channel are assumed to be independent on x ($\partial(R)/\partial x = 0$). Thus, the outflow conditions for all quantities are determined from the interior grid points of the computational domain.

The boundary conditions for Ψ are also easy implemented from (11), since the velocity components are known (fully developed flow at the entrance and no slip conditions on the plates). The value of Ψ at the entrance is $\Psi(0,y) = 2y^2 - (4/3)y^3$.

The dimensionless temperature T at the plates is also easy calculated from (9) and it is additionally assumed that in the entrance of the channel is varying linearly and is given by the expression $T(0,y) = 1 - y$.

However, in order to solve the vorticity transport equation (13) it is also necessary to determine boundary conditions of the vorticity J and this is not an easy task. It is already mentioned that at the exit no dependence on the x-direction is taken into account. Also, at the entrance the use of (10) permits the easy derivation of the corresponding boundary condition for J.

On the contrary, the derivation of boundary conditions of J on the solid surfaces (plates) is more complicated. Quartapelle and Valz-Gris [25] demonstrated that there is no strictly equivalent local boundary condition available for J. The vorticity is to be computed from the velocity field, but it cannot be specified at the boundaries before the problem is solved.

So, the solution of the problem under consideration is not as simple as it first appears to be, and special techniques are needed to utilize the numerical methods. To overcome this difficulty, at each iteration step, numerical boundary conditions are constructed for the vorticity J, using the stream function Ψ, as follows.

An arbitrary boundary grid point (i,m) is considered, as shown in Fig. 2. The vorticity is related with the stream function with the relation

$$J_{i,m} = -\left(\frac{\partial^2 \Psi}{\partial x^2} + \frac{\partial^2 \Psi}{\partial y^2}\right)_{i,m}.$$

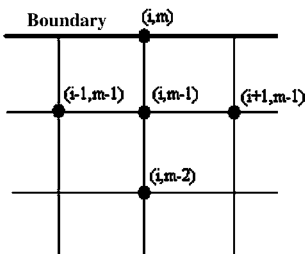

Fig. 2. Grid points for the calculation of $J_{i,m}$ at the boundary point (i,m).

Provided that the boundaries are still ($u = v = 0$), it is assumed that the $J_{i,m}$ can be expressed through the following linear combination of neighboring to (i,m) points of Ψ

$$J_{i,m} = -\left(\frac{\partial^2 \Psi}{\partial x^2} + \frac{\partial^2 \Psi}{\partial y^2}\right)_{i,m} = a_1 \Psi_{i-1,m-1} + a_2 \Psi_{i,m-1} + a_3 \Psi_{i+1,m-1} + a_4 \Psi_{i,m-2},$$

where a_k, $k = 1$–4, coefficients to be determined.

Hereafter, the terms of the stream function of the right-hand side are replaced by the corresponding expansions of Taylor series

$$\Psi_{i,m\pm n} = \Psi_{i,m} \pm n(\Delta y)\left.\frac{\partial \Psi}{\partial y}\right|_{i,m} + \frac{1}{2}n^2(\Delta y)^2\left.\frac{\partial^2 \Psi}{\partial y^2}\right|_{i,m} + ((\Delta y)^3),$$

$$\Psi_{i\pm n,m} = \Psi_{i,m} \pm n(\Delta x)\left.\frac{\partial \Psi}{\partial x}\right|_{i,m} + \frac{1}{2}n^2(\Delta x)^2\left.\frac{\partial^2 \Psi}{\partial x^2}\right|_{i,m} + ((\Delta x)^3).$$

By the solution of the system resulting from the equation of terms of the same power it turns out that the vorticity at the boundary point is calculated by the following expression

$$J_{i,m} = -\frac{(\Psi_{i+1,m-1} - 2\Psi_{i,m-1} + \Psi_{i-1,m-1})}{(\Delta x)^2} - \frac{(\Psi_{i,m-2} - \Psi_{i,m-1})}{3(\Delta y)^2}. \tag{15}$$

The vorticity boundary conditions just derived enable us to solve (13) provided that the right-hand side is already known from the previous iteration. However, the determination of Ψ from (11) depends on the distribution of vorticity within the bounded domain. Thus Ψ and J are coupled and for the solution of the system (12)–(14) an iterative procedure will employed.

4. Numerical method

For the numerical solution of the system of equations (12)–(14) an efficient technique has been developed based on a numerical method described in [26] as follows.

Eq. (12) is a Poisson equation and can be solved fast and efficiently by the use of a simple SOR method. The main effort focused on solving the other two equations of the system, namely (13) and (14).

The arising difficulty solving Eqs. (13) and (14), appearing in fluid mechanics problems, is the presence of non-linear terms like

$$\frac{\partial \Psi}{\partial y}\frac{\partial J}{\partial x} - \frac{\partial \Psi}{\partial x}\frac{\partial J}{\partial y}$$

in Eq. (13). These non-linear terms cause the diagonal dominance to be lost in the matrix associated with the approximating finite-difference equations, if one of the standard central-difference numerical schemes is used. Thus, the aim of the numerical method used, is to make the matrices of the coefficients of the unknowns diagonally dominant, so as the corresponding equations will be amenable to solution by iterative methods (i.e. SOR).

For the demonstration of the used numerical technique Eq. (13) is taken into account

$$\nabla^2 J = Re\left\{\frac{\partial J}{\partial x}\frac{\partial \Psi}{\partial y} - \frac{\partial J}{\partial y}\frac{\partial \Psi}{\partial x}\right\} + Mn\,Re\,H\left\{\frac{\partial H}{\partial x}\frac{\partial T}{\partial y} - \frac{\partial H}{\partial y}\frac{\partial T}{\partial x}\right\}. \tag{16}$$

In order to avoid the aforementioned difficulty Eq. (16) can be split into two equations, namely

$$\frac{\partial^2 J}{\partial x^2} - Re\,u\frac{\partial J}{\partial x} = G_1(x,y) + A(x,y), \tag{17}$$

$$\frac{\partial^2 J}{\partial y^2} - Re\,v\frac{\partial J}{\partial y} = -A(x,y), \tag{18}$$

where, $A(x,y)$ is an unknown function and

$$G_1(x,y) = Mn\,Re\,H\left\{\frac{\partial H}{\partial x}\frac{\partial T}{\partial y} - \frac{\partial H}{\partial y}\frac{\partial T}{\partial x}\right\}.$$

The next step is to consider the local transformation for Eq. (17) for $x_0 - \Delta x \leqslant x \leqslant x_0 + \Delta x$ and y equal to y_0

$$J(x,y_0) = P(x,y_0)e^{[-c(x,y_0)]}, \quad \text{where } c(x,y_0) = -\frac{Re}{2}\int_{x_0}^{x} u(x,y_0)\,\mathrm{d}x \tag{19}$$

and $P(x,y_0)$ is an unknown function.

Similarly, the local transformation for $y_0 - \Delta y \leqslant y \leqslant y_0 + \Delta y$, for Eq. (18) is considered, this time, for x equal to x_0

$$J(x_0,y) = S(x_0,y)e^{[-q(x_0,y)]}, \quad \text{where } q(x_0,y) = -\frac{Re}{2}\int_{y_0}^{y} v(x_0,y)\,\mathrm{d}y \tag{20}$$

and $S(x_0,y)$ is an unknown function.

Thus, substitution of (19) to (17) and (20) to (18) gives the following system of equations

$$\frac{\partial^2 P}{\partial x^2} + \left(\frac{Re}{2}\frac{\partial u}{\partial x} - \frac{Re^2u^2}{4}\right)P = [G_1(x,y_0) + A(x,y_0)]e^{c(x,y_0)}, \tag{21}$$

$$\frac{\partial^2 S}{\partial y^2} + \left(\frac{Re}{2}\frac{\partial v}{\partial y} - \frac{Re^2v^2}{4}\right)S = -A(x_0,y)e^{q(x_0,y)}. \tag{22}$$

By descretizing equations the second order derivatives of (21) and (22) with central-difference approximations at the point (x_0,y_0), eliminating $A(x_0,y_0)$, between the two new equations and substituting P and S by their appropriate expressions (19) and (20) at the corresponding points around (x_0, y_0), it is obtained that

$$J_1 e^{c_1} + J_3 e^{c_3} + \lambda^2 J_2 e^{q_2} + \lambda^2 J_4 e^{q_4} + \left(-2 + \frac{Re(\Delta x)^2}{2} \frac{\partial u}{\partial x}\bigg|_0 - \frac{Re^2 u_0^2 (\Delta x)^2}{4} - 2\lambda^2 \right.$$
$$\left. + \frac{Re(\Delta x)^2}{2} \frac{\partial v}{\partial y}\bigg|_0 - \frac{Re^2 v_0^2 (\Delta x)^2}{4} \right) J_0 = (\Delta x)^2 G_1(x_0, y_0) + \mathrm{O}((\Delta x)^4) + \mathrm{O}((\Delta x)^2 (\Delta y)^2), \quad (23)$$

where, Δx and Δy is the Cartesian mesh size at the x- and y-direction, respectively and $\lambda = \Delta x/\Delta y$. The number of grid points is M, N at the x- and y-direction, respectively. By the subscripts 0, 1, 2, 3 and 4 it is denoted the typical set of grid points (x_0, y_0), $(x_0 + \Delta x, y_0)$, $(x_0, y_0 + \Delta y)$, $(x_0 - \Delta y, y_0)$ and $(x_0, y_0 - \Delta y)$, respectively.

However, the matrix of unknowns associated with (23) is not necessarily diagonally dominant, which is a prerequisite for the convergence of the iterative procedure. Diagonal dominance is obtained by expanding the exponential terms in Taylor series at the point (x_0, y_0) and keeping the sufficient number of terms so that the order of the truncation error is conserved.

So, $u(x, y)$ is expanded in Taylor series at the point (x_0, y_0) in the direction of x increasing, so that Eq. (19) can be integrated to give $c(x, y_0)$ in powers of $(x - x_0)$. The c_1 and c_3 are obtained in powers of Δx if in this latter equation is set successively $x = x_0 + \Delta x$ and $x = x_0 - \Delta x$, respectively.

The values of c_1 and c_3 are used for the calculation of e^{c_1} and e^{c_3} in the form of Taylor series, which will be substituted in the first two terms of the left-hand side of Eq. (23). The same procedure is followed to deduce likewise expressions for the other two terms of the left-hand side member of Eq. (23). In this way and using the equation of continuity (1), Eq. (16) finally takes the form

$$k_1 J_1 + k_2 J_2 + k_3 J_3 + k_4 J_4 + k_0 J_0 = (\Delta x)^2 G_1(x_0, y_0), \quad (24)$$

where,

$$k_1 = 1 + \frac{Re^2 u_0^2}{8} (\Delta x)^2 - \frac{Re u_0}{2} (\Delta x), \quad k_2 = \lambda^2 \left[1 + \frac{Re^2 v_0^2}{8} (\Delta y)^2 - \frac{Re v_0}{2} (\Delta y) \right],$$

$$k_0 = -2 - \frac{Re^2 u_0^2 (\Delta x)^2}{4} - 2\lambda^2 - \frac{Re^2 v_0^2 (\Delta x)^2}{4},$$

$$k_3 = 1 + \frac{Re^2 u_0^2}{8} (\Delta x)^2 + \frac{Re u_0}{2} \Delta x, \quad k4 = \lambda^2 \left[1 + \frac{Re^2 v_0^2}{8} (\Delta y)^2 + \frac{Re v_0}{2} (\Delta y) \right].$$

Similarly, for Eqs. (12) and (14) it is obtained that

$$p_1 \Psi_1 + p_2 \Psi_2 + p_3 \Psi_3 + p_4 \Psi_4 + p_0 \Psi_0 = -(\Delta x)^2 J_0, \quad (25)$$

where,

$$p_1 = 1, \quad p_2 = \lambda^2, \quad p_3 = 1, \quad p_4 = \lambda^2, \quad p_0 = -2 - 2\lambda^2.$$

$$d_1 T_1 + d_2 T_2 + d_3 T_3 + d_4 T_4 + d_0 T_0 = (\Delta x)^2 G_2(x_0, y_0), \tag{26}$$

where,

$$G_2(x_0, y_0) = Mn\, Pr\, Re\, Ec\, H\, \varepsilon \left\{ \frac{\partial H}{\partial x}\frac{\partial \Psi}{\partial y} - \frac{\partial H}{\partial y}\frac{\partial \Psi}{\partial x} \right\} + Pr\, Ec \left[\left(\frac{\partial^2 \Psi}{\partial y^2} - \frac{\partial^2 \Psi}{\partial x^2} \right)^2 + 4\left(\frac{\partial^2 \Psi}{\partial x \partial y} \right)^2 \right],$$

$$d_1 = 1 + \frac{Re^2\, Pr^2\, u_0^2}{8}(\Delta x)^2 - \frac{Re\, Pr\, u_0}{2}(\Delta x), \quad d_2 = \lambda^2 \left[1 + \frac{Re^2\, Pr^2\, v_0^2}{8}(\Delta y)^2 - \frac{Re\, Pr\, v_0}{2}(\Delta y) \right],$$

$$d_0 = -2 - \frac{Re^2\, Pr^2\, u_0^2 (\Delta x)^2}{4} - 2\lambda^2 - \frac{Re^2\, Pr^2\, v_0^2 (\Delta x)^2}{4} + Mn\, Pr\, Re\, Ec\, H \left\{ \frac{\partial H}{\partial x}\frac{\partial \Psi}{\partial y} - \frac{\partial H}{\partial y}\frac{\partial \Psi}{\partial x} \right\} (\Delta x)^2,$$

$$d_3 = 1 + \frac{Re^2\, Pr^2\, u_0^2}{8}(\Delta x)^2 + \frac{Re\, Pr\, u_0}{2}\Delta x, \quad d_4 = \lambda^2 \left[1 + \frac{Re^2\, Pr^2\, v_0^2}{8}(\Delta y)^2 + \frac{Re\, Pr\, v_0}{2}(\Delta y) \right].$$

The linear systems (24)–(26) are sparse and the matrices associated with them are always diagonally dominant since the coefficients of the unknowns satisfy the conditions [27]

$$\sum_{\substack{j=1 \\ j \neq i}}^{N \times M} |k_{ij}| \leqslant |k_{ii}|, \quad \sum_{\substack{j=1 \\ j \neq i}}^{N \times M} |m_{ij}| \leqslant |m_{ii}|, \quad \sum_{\substack{j=1 \\ j \neq i}}^{N \times M} |d_{ij}| \leqslant |d_{ii}|, \quad i = 1, 2, \ldots, N \times M.$$

Having assured that the descretization of each of the equations of the system (12)–(14) leads to an algebraic system with diagonally dominant matrices it is now possible to proceed to the solution of the aforementioned system, subjected to the boundary conditions described in Section 3.1.

The solution is obtained by using an iterative procedure. An under relaxation technique was used for (24) and (25) whereas, an SOR was used for (26). The under relaxation parameter was chosen to be 0.7 and the over relaxation one 1.2.

The steps of the procedure followed are

- Give initial guesses for the interior points of the computational domain and the boundary conditions.
- Calculate a new estimation for Ψ by solving (24) once, considering J known.
- Considering Ψ known construct the boundary conditions for J using (15).
- Calculate a new estimation for J by solving (25) once, considering Ψ, T known.
- Considering now Ψ and J known, calculate a new estimation for T by solving (26) once.
- Compare the new estimation with the old ones. If the criterion of convergence is not satisfied set the new estimations old and return to the second step.

The criterion of convergence used is

$$\frac{1}{MN}\sum_{i=1}^{M}\sum_{j=1}^{N}|F^{n+1}-F^{n}|<10^{-5},$$

where, F^n is an estimation of an unknown function F, (Ψ, J or T) at the n iteration.

5. Results and discussion

In order to study the biomagnetic fluid flow, in the rectangular channel, under the influence of an applied magnetic field, the above described numerical technique was applied to solve the system of equations (12)–(14), under the appropriate boundary conditions.

For the numerical solution it is necessary to assign values in the dimensionless parameters entering into the problem under consideration. For this purpose a realistic case is considered in which the fluid is the blood ($\bar{\rho}=1050\ \mathrm{kg\,m^{-3}}$, $\bar{\mu}=3.2\times10^{-3}\ \mathrm{kg\,m^{-1}\,s^{-1}}$) [28], flowing with maximum velocity $\bar{u}_r=3.81\times10^{-2}\ \mathrm{m\,s^{-1}}$ and the plates are located at distance $\bar{h}=2.0\times10^{-2}$ m. In this case the Reynolds number, Re, is equal to 250.

The new dimensionless parameter appearing in the problem is the magnetic number Mn and it can written as

$$Mn=\frac{\bar{\mu}_0\overline{H}_r^2\overline{K}(\overline{T}_\mathrm{u}-\overline{T}_1)}{\bar{\rho}\bar{u}_r^2}=\frac{\bar{\mu}_0\overline{H}_r\overline{K}\overline{H}_r(\overline{T}_\mathrm{u}-\overline{T}_1)}{\bar{\rho}\bar{u}_r^2}=\frac{\overline{B}_r\overline{M}_r}{\bar{\rho}\bar{u}_r^2},\tag{27}$$

where $\overline{B}_r$ and $\overline{M}_r$ are the magnetic induction and the magnetization at the point $(2.5,0)$, respectively. For magnetic field 8 T, the blood has reached magnetization of 60 A/m [4].

From the definition of the Reynolds number it is also obtained that $\bar{u}_r=\bar{\mu}Re/\bar{h}\bar{\rho}$ and substitution of this relation to (27) gives

$$Mn=\frac{\overline{M}_r\overline{B}_r\bar{h}^2\bar{\rho}}{\bar{\mu}^2Re^2}.\tag{28}$$

From (28) it is derived that the corresponding Mn for magnetic field strength 8 T at the point $(2.5,0)$ is $Mn\approx315$.

It is also considered that the temperature of the plates to be $\overline{T}_\mathrm{u}=43$ °C whereas $\overline{T}_1=3.5$ °C. For these values of plate temperatures the temperature number ϵ is equal to 8.

Although the viscosity $\bar{\mu}$, the specific heat under constant pressure $\bar{c}_p$ and the thermal conductivity $\bar{k}$ of any fluid, and hence of the blood, are temperature dependent, Prandtl number can be considered constant. Thus, for the temperature range considered in this problem, the value of $\bar{c}_p$ and $\bar{k}$ is equal to 14.65 $\mathrm{J\,kg^{-1}\,K^{-1}}$ and $2.2\times10^{-3}\ \mathrm{J\,m^{-1}\,s^{-1}\,K^{-1}}$, respectively, [29,30] and hence it can be considered that $Pr=20$. For these values of the parameters it is also derived that the Eckert number $Ec=2.476\times10^{-6}$.

The present results where obtained for $\Delta x = \Delta y = 0.02$, i.e. 38,301 grid points. Calculations where made also for $\Delta x = \Delta y = 0.012$, i.e. 70,056 grid points and no significant differences where found.

For the above mentioned values of the dimensionless parameters the obtained results are shown in Figs. 3–6 concerning the velocity field, the temperature field and the coefficients of skin friction and rate of heat transfer.

Figs. 3 and 4 show the stream and vorticity function contours, respectively, for the values of the above mentioned parameters and for magnetic numbers $Mn = 315$, 215 and 115. It is observed that a vortex is arising at the area where the magnetic source is located. As the magnetic number

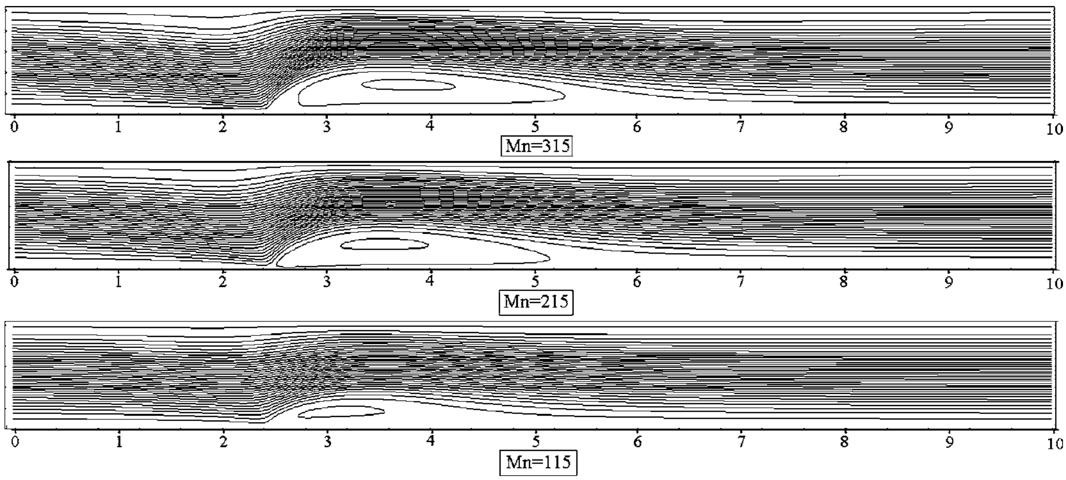

Fig. 3. Stream function contours for $Re = 250$.

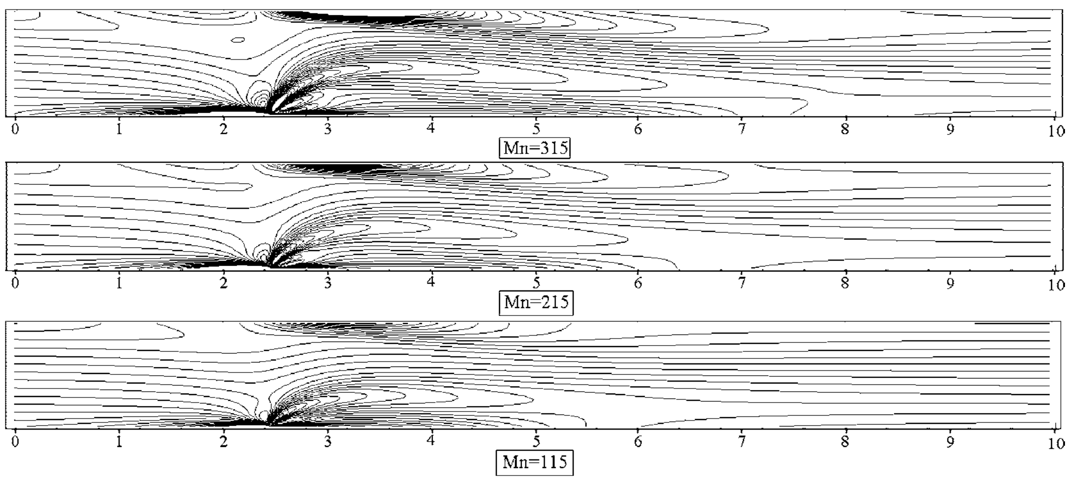

Fig. 4. Vorticity function contours for $Re = 250$.

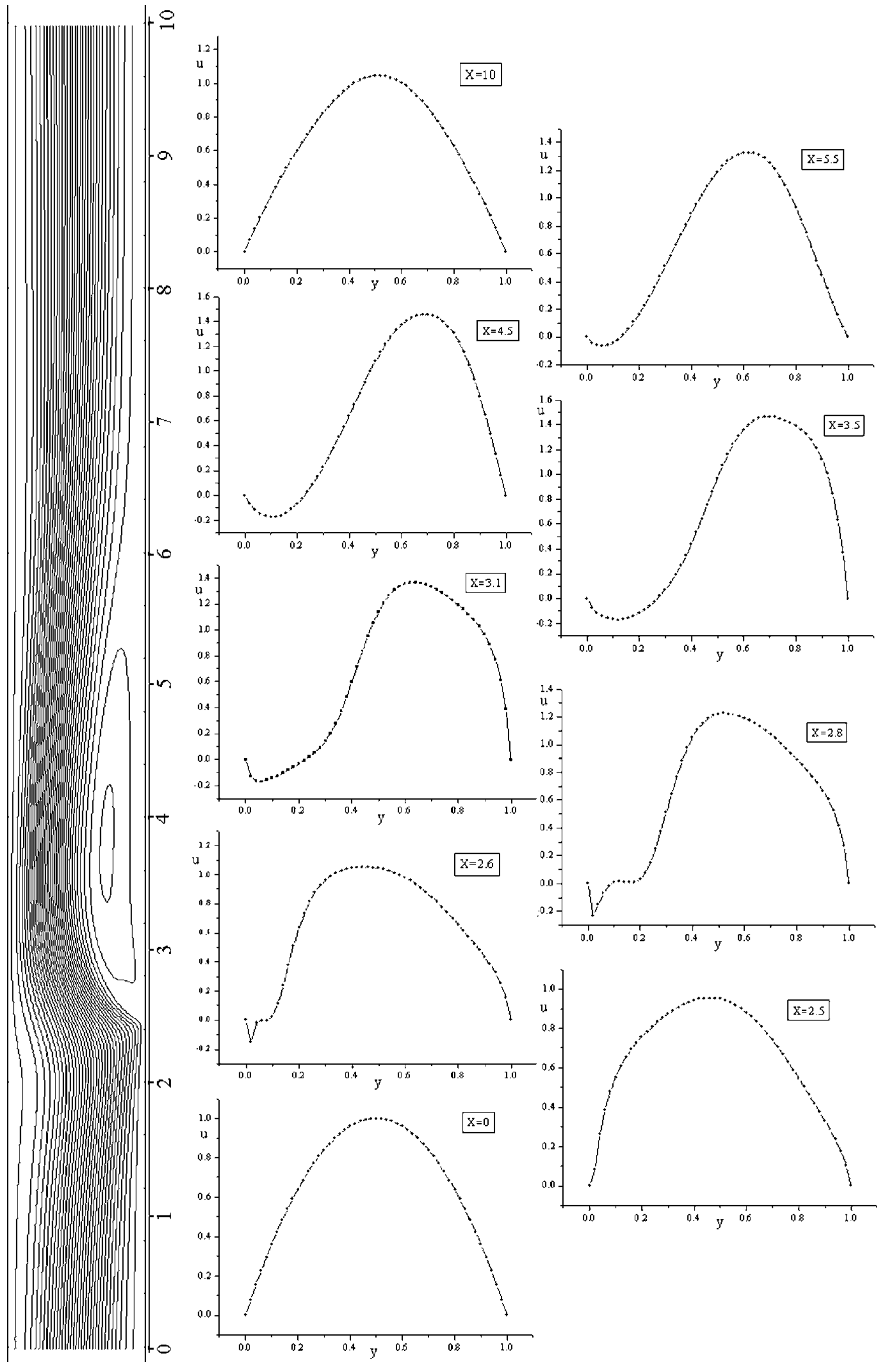

Fig. 5. Stream function contours and velocity profiles at various positions for $Mn = 315$ and $Re = 250$.

increases, which means increment of the magnetic field strength at the source, as long as the temperature difference is fixed, the vortex is extended.

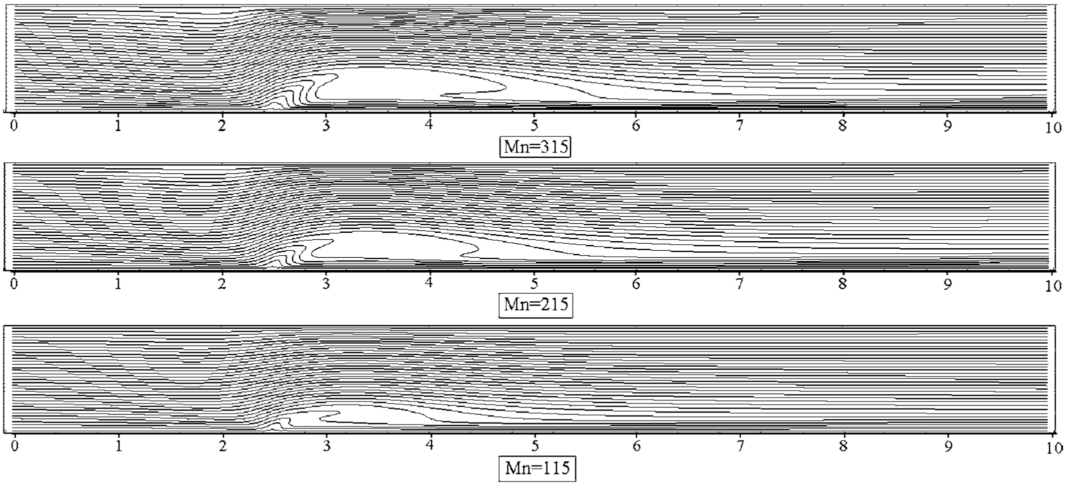

Fig. 6. Contours of the dimensionless temperature T for $Mn = 315$ and $Re = 250$.

It should be remarked that in the absence of the magnetic field ($Mn = 0$) the stream function as well as the vorticity function contours are straight lines and the velocity profile u is the same with the one shown at the entrance of the duct in Fig. 5.

The profiles of the dimensionless velocity component u along specific locations in the channel are shown in Fig. 5. At the point $x = 2.6$ the flow is separated from the wall and at $x \approx 3.1$, reattaches with the lower plate. Finally, the flow at the exit $x = 10$ is again reverted to fully developed.

The dimensionless temperature contours for the same values of the magnetic number Mn are shown in Fig. 6. It is observed an increment in the temperature of the biofluid near the lower plate where the source is located. For $Mn = 315$, the variation of dimensional temperature, at different positions in the channel as well as the corresponding contours, are shown in Fig. 7. The disturbance in the flow field due to the magnetic source is transferred very far downstream. As a result, the profile of the temperature at the exit of the channel differs slightly than that of the entrance. Calculations were made also for $\bar{L}/\bar{h} = 12, 15$ and 20 to verify this behavior and the last dimensional temperature profile pictured in Fig. 7 is at $x = 15$. It is noted that in the absence of magnetic field the contours of temperature are straight, equally spaced, lines.

The most important flow and heat transfer characteristics are the local skin friction coefficient and the local rate of heat transfer coefficient. These quantities can be defined by the following relations

$$C_\mathrm{f} = \frac{2\bar{\tau}_1}{\bar{\rho}\bar{u}_r^2}, \quad Nu = \frac{\bar{q}\bar{h}}{\bar{k}(\overline{T}_\mathrm{u} - \overline{T}_1)}, \tag{29}$$

where, $\bar{\tau}_1 = \bar{\mu}(\partial\bar{u}/\partial\bar{y})|_{\bar{y}=0,\bar{h}}$ is the wall shear stress and the heat flux between the fluid and the plates is $\dot{\bar{q}} = -\bar{k}(\partial\overline{T}/\partial\bar{y})|_{\bar{y}=0,\bar{h}}$.

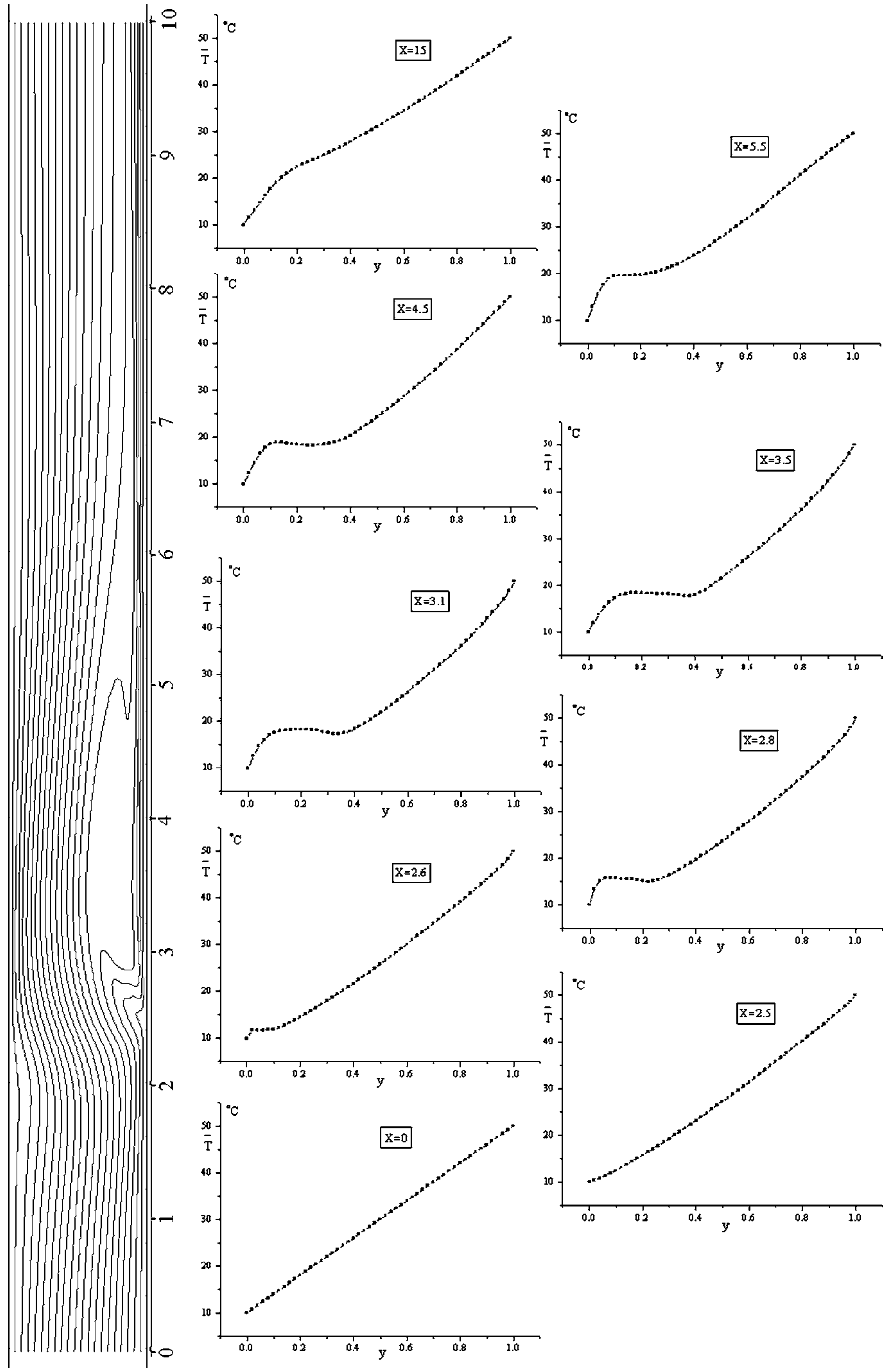

Fig. 7. Dimensional temperature contours and profiles profiles at various positions for $Mn = 315$ and $Re = 250$.

By the use of (8), (11) the above mentioned quantities can be written as

$$C_{\mathrm{f}} = \left.\frac{2\Psi''(x,y)}{Re}\right|_{y=0,1}, \quad Nu = \left.\frac{\partial T}{\partial y}\right|_{y=0,1} = T'(x,y)|_{y=0,1}, \tag{30}$$

where Nu is the Nusselt number, $\Psi''(x,y)|_{y=0,1}$ is the dimensionless wall shear parameter and $T'(x,y)|_{y=0,1}$ is the dimensionless wall heat transfer parameter.

The variation of these mentioned dimensionless parameters, for $Mn = 115$, 215 and 315, are shown in Figs. 8–11. The wall shear as well as the heat transfer parameters are more influenced on the lower plate, below of which the magnetic source is located. It is remarkable that the variation of each one of these parameters is qualitatively the same as the Mn varies from 115 to 315. The increment of Mn results to greater variations of these parameters.

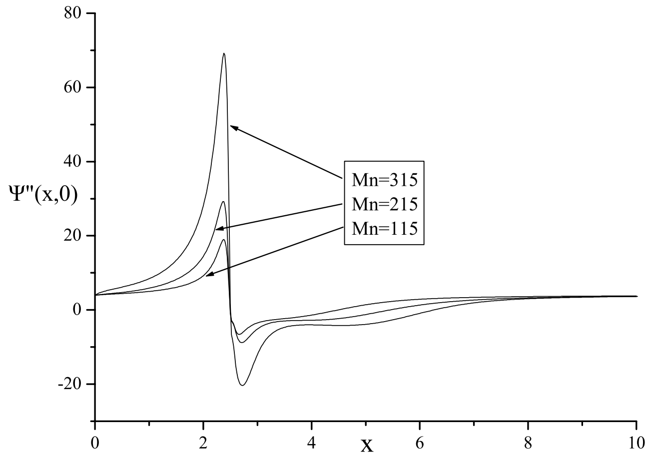

Fig. 8. Skin friction coefficient of the lower plate for $Re = 250$.

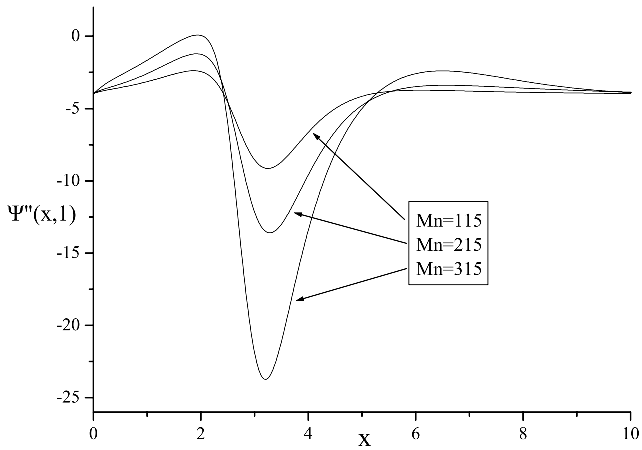

Fig. 9. Skin friction coefficient of the upper plate for $Re = 250$.

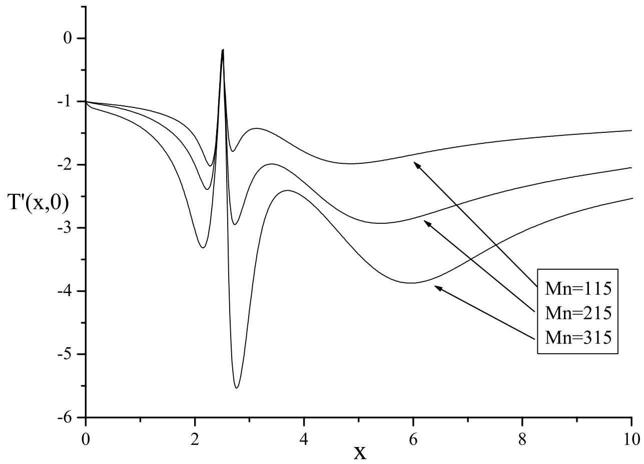

Fig. 10. Heat transfer parameter of the lower wall for $Re = 250$.

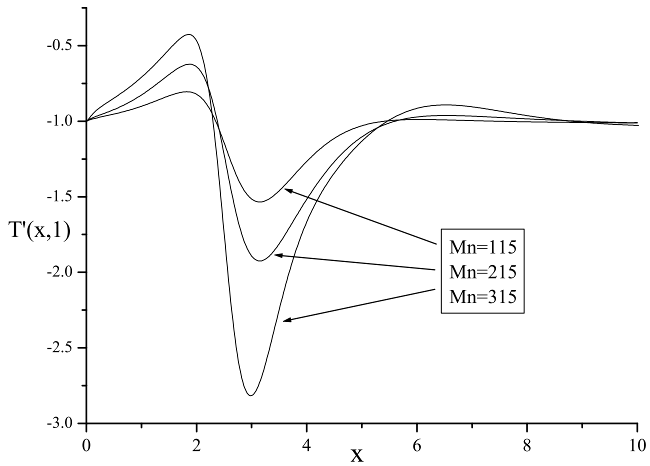

Fig. 11. Heat transfer parameter of the upper wall for $Re = 250$.

The dimensionless wall shear parameter of the lower wall $\Psi''(x,y)|_{y=0}$ is pictured in Fig. 8 for the aforementioned values of the Mn.

The value of the parameter increases rapidly in the region $x = 1.5$–2.38, where it reaches its maximum value. Very close to the region where the source is located ($x = 2.5$), a corresponding decrement take place and at $x = 2.72$ this parameter takes its minimum negative value.

Fig. 9 shows the variation of the wall shear parameter of the upper plate $\Psi''(x,y)|_{y=1}$. This parameter increases near the area of the magnetic source in a smoother way and it's sign does not change as happens with the lower plate where reverse of the flow occurs.

From the Figs. 8 and 9 can be observed that far downstream, $x = 10$, the wall shear parameter of both plates, reach its original value $x = 0$ corresponding to fully developed flow. An another important information that can be obtained, is the points where these parameters are take zero values. This happens only for the lower plate for two points, $x = 2.5$ for all Mn, and $x = 6.27$, 5.45 and 4.49 for Mn 315, 215 and 115, respectively. In these points there is no skin friction and this result may be interesting in the case of creation of fibrinoid.

With the use of the wall shear parameter and the relations (29) and (30) it is possible to calculate the drag D_l and D_u acting on the lower and upper plate, respectively. Provided that the width of the plates is considered unity, the drag is given by the relation

$$\overline{D}_{l,u} = \int_0^{\bar{L}} \bar{\tau}_l|_{y=0,\bar{h}}\,\mathrm{d}\bar{x} = \frac{\bar{\rho}\bar{h}\bar{u}_r^2}{Re}\int_0^{10} \Psi''(x,y)|_{y=0,1}\,\mathrm{d}x. \tag{31}$$

Calculation of the above mentioned integrals gives that $D_u/D_l = 55.85/34.17$. Consequently, the drag acting on the upper plate increases 63.45% more than that of the lower.

Figs. 10 and 11 show the variation of the heat transfer parameter for the lower and upper plate, respectively. Analogous variation is observed, for this parameter, for both plates, but in this case, far downstream the value of $T'(x,0)$ or $T'(x,1)$ do not reach their original values. This happens because, as already mentioned, the disturbance of the temperature field is extended far downstream.

The rate of heat transfer between a plate and the biofluid, i.e. the thermal energy convected from a plate to the fluid or reversely, per unit area and per unit time ($\mathrm{J\,m^{-2}\,s^{-1}}$) is given from the Fourier law of thermal conductivity

$$\dot{q}_{\mathrm{wall}} = -\bar{k}\left(\frac{\partial\overline{T}}{\partial\bar{y}}\right)_{\bar{y}=0,\bar{h}} = \bar{k}\frac{\overline{T}_u - \overline{T}_l}{\bar{h}}\left(\frac{\partial T}{\partial y}\right)_{y=0,1}. \tag{32}$$

For the lower plate and Fig. 10 can be observed that $\partial T/\partial y|_{y=0} < 0$ thus $\dot{q}_{\mathrm{wall}} < 0$ and the heat flows from the fluid to the plate. Similarly, for the upper plate and Fig. 11 obtained that $\partial T/\partial y|_{y=0} < 0$ and $\dot{q}_{\mathrm{wall}} < 0$ and the heat flows from the plate to the biofluid.

From relation (32) is possible to calculate the thermal energy Q_u and Q_l convected from the upper plate to the fluid and from the fluid to the lower plate, respectively. Provided that the width of the plates is unity the convected thermal energy is given by the relation

$$Q_{u,l} = \int_0^{\bar{L}} \dot{q}_{\mathrm{wall}}\,\mathrm{d}\bar{x} = \bar{k}(\overline{T}_u - \overline{T}_l)\int_0^{10} \left.\frac{\partial T}{\partial y}\right|_{y=0,1}\mathrm{d}x. \tag{33}$$

By calculation of the above mentioned integrals it is obtained that $Q_l/Q_u = 28.56/11.55$. Consequently, the thermal energy convected from the fluid to the lower plate is 147.27% more than that convected from the upper plate to the fluid. This difference occurs, primarily in the presence of the magnetic field.

6. Conclusions

The biomagnetic fluid flow in a channel is studied under the influence of an applied magnetic field. A vortex is arising at the area where the magnetic source is located. This phenomenon is extended as the magnetic field strength further increases. The temperature also increases at the same area. The skin friction coefficient as well as the rate of heat transfer at the walls, especially at the lower plate, are also increased with the increment of the magnetic field strength. The above mentioned results indicate that the application of a magnetic field, appreciably influences the flow of a biomagnetic fluid and should be further studied for possible useful medical and engineering applications.

Acknowledgement

This work was partially supported by the No. 2439 Karatheodoris program of the Research Committee, University of Patras.

References

[1] J.M.R. Carlton, C.A. Yowell, K.A. Sturrock, J.B. Dame, Biomagnetic separation of contaminating host leukocytes from plasmodium-infected erythrocytes, Experimental Parasitology 97 (2001) 111–114.
[2] C.B. Fuh, L.Y. Lin, M.H. Lai, Analytical magnetapheresis of magnetically susceptible particles, Journal of Chromatography A 874 (2000) 131–142.
[3] P.A. Voltairas, D.I. Fotiadis, L.K. Michalis, Hydrodynamics of magnetic drug targeting, Journal of Biomechanics 35 (2002) 813–821.
[4] Y. Haik, V. Pai, C.J. Chen, Development of magnetic device for cell separation, Journal of Magnetism and Magnetic Materials 194 (1999) 254–261.
[5] V. Badescou, O. Rotariu, V. Murariu, N. Rezlescu, Transverse high gradient magnetic filter cell with bounded flow field, IEEE Transactions on Magnetics 33 (6) (1997) 4439–4444.
[6] E.K. Ruuge, A.N. Rusetski, Magnetic fluid as drug carriers: targeted transport of drugs by a magnetic field, Journal of Magnetism and Magnetic Materials 122 (1993) 335–339.
[7] J. Plavins, M. Lauva, Study of colloidal magnetite binding erythrocytes: prospects for cell separation, Journal of Magnetism and Magnetic Materials 122 (1993) 349–353.
[8] Y. Haik, J.C. Chen, V.M. Pai, Development of bio-magnetic fluid dynamics, in: S.H. Winoto, Y.T. Chew, N.E. Wijeysundera (Eds.), Proceedings of the IX International Symposium on Transport Properties in Thermal Fluids Engineering, Singapore, Pacific Center of Thermal Fluid Engineering, Hawaii, USA, June 25–28, 1996, pp. 121–126.
[9] Y. Haik, V. Pai, C.J. Chen, Biomagnetic fluid dynamics, in: W. Shyy, R. Narayanan (Eds.), Fluid Dynamics at Interfaces, Cambridge University Press, 1999, pp. 439–452.
[10] V.G. Bashtovoy, B.M. Berkovsky, A.N. Vislovich, Introduction to Thermomechanics of Magnetic Fluids, Hemisphere Publishing Co., Springer-Verlang, 1988.
[11] B. Berkovski, V. Bashtovoy, Magnetic Fluids and Applications Handbook, Begell House Inc., New York, 1996.
[12] E. Blums, A. Cebers, M.M. Maiorov, Magnetic Fluids, Walter de Gruyter, Berlin, 1997.
[13] V.E. Fertman, Magnetic Fluids Guidebook: Properties and Applications, Hemisphere Publishing Co., New York, 1990.
[14] J.L. Neuringer, R.E. Rosensweig, Ferrohydrodynamics, Physics of Fluids 7 (1964) 1927–1937.
[15] R.E. Rosensweig, Ferrohydrodynamics, Cambridge University Press, 1985.
[16] R.E. Rosensweig, Magnetic fluids, Annual Review of Fluid Mechanics 19 (1987) 437–463.
[17] T. Higashi, A. Yamagishi, T. Takeuchi, N. Kawaguchi, S. Sagawa, S. Onishi, M. Date, Orientation of erythrocytes in a strong static magnetic field, Journal of Blood 82 (4) (1993) 1328–1334.
[18] A.N. Shaylgin, S.B. Norina, E.I. Kondorsky, Behavior of erythrocytes in high gradient magnetic field, Journal of Magnetism and Magnetic Materials 31 (1983) 555–556.

[19] T. Takeuchi, T. Mizuno, A. Yamagishi, T. Higashi, M. Date, Orientation of red blood cells in high magnetic field, Journal of Magnetism and Magnetic Materials 140–144 (2) (1995) 1462–1463.
[20] T. Higashi, N. Ashida, T. Takeuchi, Orientation of blood cells in static magnetic field, Physica B (1997) 616–620.
[21] L. Pauling, C.D. Coryell, The magnetic properties and structure of hemoglobin, oxyhemoglobin and carbonmonoxy hemoglobin, in: Proceedings of the National Academy of Science, USA, 22, 1936, pp. 210–216.
[22] G.R. Zendehbudi, M.S. Moayeri, Comparison of physiological and simple pulsatile flows through stenosed arteries, Journal of Biomechanics 32 (1999) 959–965.
[23] H.I. Andersson, R. Halden, T. Glomsaker, Effects of surface irregularities on flow resistance in differently shaped arterial stenoses, Journal of Biomechanics 33 (10) (2000) 1257–1262.
[24] H. Matsuki, K. Yamasawa, K. Murakami, Experimental considerations on a new automatic cooling device using temperature sensitive magnetic fluid, IEEE Transactions on Magnetics 13 (5) (1977) 1143–1145.
[25] L. Quartapelle, F. Valz-Gris, Projection conditions on the vorticity in viscous incompressible flows, International Journal for Numerical Methods in Fluids 1 (2) (1981) 129–144.
[26] V.C. Loukopoulos, A difference method for solving the Navier–Stokes equations for axisymmetric flow, in: Proceedings of 4th GRACM Congress on Computational Mechanics, Patras, Greece, 1, 2002, pp. 88–95.
[27] K. Atkinson, An Introduction to Numerical Analysis, John Wiley and Sons, New York, 1992.
[28] T.J. Pedley, The Fluid Mechanics of Large Blood Vessels, Cambridge University Press, 1980.
[29] J.C. Chato, Heat tranfer to blood vessels, Journal of Biomechanical Engineering 102 (1980) 110–118.
[30] J.W. Valvano, S. Nho, G.T. Anderson, Analysis of the Weinbaum–Jiji model of blood flow in the canine kidney cortex for self-heated thermistors, Journal of Biomechanical Engineering 116 (2) (1994) 201–207.